Magnetism and half-metallicity at the O surfaces of ceramic oxides

S. Gallego, J.I. Beltrán, J. Cerdá, and M.C. Muñoz
Instituto de Ciencia de Materiales de Madrid,
Consejo Superior de Investigaciones Científicas,
Cantoblanco, 28049 Madrid, Spain
(Dated: initially submitted 9 February)

The occurence of spin-polarization at ZrO_2, Al_2O_3 and MgO surfaces is proved by means of *ab-initio* calculations within the density functional theory. Large spin moments, as high as 1.56 μ_B, develop at O-ended polar terminations, transforming the non-magnetic insulator into a half-metal. The magnetic moments mainly reside in the surface oxygen atoms and their origin is related to the existence of $2p$ holes of well-defined spin polarization at the valence band of the ionic oxide. The direct relation between magnetization and local loss of donor charge makes possible to extend the magnetization mechanism beyond surface properties.

PACS numbers: 75.70.Rf, 75.70.-i, 73.20.At, 73.20.-r, 85.75.-d

When dimensions are reduced to the nanoscale, we are faced to a new understanding of the physical properties of matter: bulk insulators and semiconductors exhibit metallic surfaces [1], non-magnetic materials get spin polarization when forming nanoparticles [2], unstable bulk structures exist in ultrathin film form [3, 4], etc. At the origin of these phenomena are the reduced dimensionality and the enhanced role of the surfaces or boundaries in the final properties of the system. Together with its inherent fundamental interest, this has important technological consequences, auspicating the birth of new technologies [5, 6]. Special attention is devoted to magnetic low dimensional structures, in particular as sources of spin current in the emerging field of spintronics [5].

In this letter, we report on the existence of large magnetic moments and half-metallicity at the O-rich surfaces of ceramic oxides, focusing on ZrO_2, Al_2O_3 and MgO. These are non-magnetic ionic insulators widely applied in bulk and thick film form, that have also been grown as ultrathin films and nanometric grains [7]. Their electronic structure can be roughly described as a valence band formed by the filled O $2p$ orbitals and a conduction band formed by the empty metal levels. When a M_xO_y unit -M being the metal donor and x,y accounting for the particular metal to oxygen ratio- is broken to form the surface, the loss of coordination of the surface O atoms originates $2p$ holes in the valence band of the oxide. Our results show that this generates high spin moments at the topmost O layer, which induce magnetization at the adjacent planes and, remarkably, alter the electronic structure of the oxide from insulating to half-metallic.

Very recently unexpected ferromagnetism has been measured in thin films of undoped non-magnetic oxides, like HfO_2 and ZrO_2, possibly assigned to the presence of lattice defects concentrated at the film interface. [8, 9]. Here we prove the existence of a magnetization mechanism rooted in the loss of donor charge of the O atoms, something that can also occur in films with cation vacancies. This provides an explanation for the origin of the magnetic moments of these so called 'd-zero' ferromagnets. Furthermore, we predict that this kind of magnetism can be extended to a wider class of non-magnetic oxides, like MgO and Al_2O_3, where the cation is not necessarily a d metal.

The presence of defects has already been found to transform certain bulk ionic materials from insulating non-magnetic to ferromagnetic: either by adding transition metal dopants [10], as occurs with TiO_2, SnO_2 and ZnO, or by a kind of molecular Hund's rule coupling for the solid state [11], as in the case of dilute divalent Ca vacancies in CaO and dilute neutral B_6 vacancies in the hexaborides. [12]. Although the magnetization mechanism reported here has an electrostatic origin similar to the one proposed in bulk CaO, new ingredients are present: the localization of the spin moments close to the surface, and the extended character of the polarized $2p$ valence band states. This suggests that intrinsically low-dimensional structures of the oxides considered, such as grains or ultrathin films, can be magnetic.

Our results are obtained from first-principles spin-polarized calculations within the DFT (density functional theory) under the GGA (generalized gradient approximation) for exchange and correlation [13]. For highly correlated systems such as transition metal oxides (TMO), this approach predicts too small magnetic moments and inaccurate magnetic energies due to its failure in describing the localized nature of the d electrons [14]. However, this is not the situation for the ceramic oxides considered here, with a valence band formed by O $2p$ orbitals. In fact, there are no valence d electrons in MgO and Al_2O_3, while it is widely recognized the success of the DFT-GGA formalism, with and without self-energy corrections [15], to determine the structural and electronic properties of ZrO_2, which are in excellent agreement with experiments [16]. We use the SIESTA package [17] with basis sets formed by double-zeta polarized localized numerical atomic orbitals. More details about the conditions of the calculations can be found elsewhere [18].

We have studied binary insulating oxides of different crystal structures: MgO, Al_2O_3 and ZrO_2, for which few calculations have considered the possibility of spin polarization at clean surfaces or in defective structures[4]. MgO adopts the rock-salt lattice, the corresponding (111) surfaces consisting of a stacking of alternated pure Mg and O planes. α-Al_2O_3 can be viewed as an hexagonal close-packed array of O atoms with the Al atoms occupying two thirds of the interstitial octahedral sites. Along the [0001] direction, consecutive O planes are separated by two Al layers. ZrO_2 displays three polymorphs at room temperature [19], either in its pure form (m-ZrO_2, monoclinic), or by dopage with substitutional cations (t-ZrO_2, tetragonal, and c-ZrO_2, cubic). The cubic structure corresponds to the CaF_2 lattice, which along the (111) direction leads to three possible terminations, labelled according to the composition of the two topmost layers: *O-O-*, *O-Zr-* and *Zr-O-*. t-ZrO_2 can be obtained from the cubic unit cell elongating one of the equivalent edges of the cube and introducing small opposite shifts at the O sublattice positions. The m-ZrO_2 lattice is more complex, but along the [001] direction it defines a layered structure of chemical stacking sequence O-O-Zr. Here we have considered all low-index terminations of c-ZrO_2, and selected t-ZrO_2, m-ZrO_2, MgO and Al_2O_3 surfaces. Each surface is modelled as a periodic slab containing a vacuum region of 10 $\mathring{A}$. The width of the vacuum region is enough to inhibit interaction between neighbouring surfaces. The number of M_xO_y units in a slab depends on the particular structure, and ranges from 5 to 7. The slabs are symmetric about the central plane, to avoid an artificial divergent Madelung energy, although we have verified that all the conclusions of this work remain unaltered if asymmetric slabs are considered instead. Bulk-like behaviour is attained at the innermost central layers. The atomic positions are allowed to relax until the forces on the atoms are less than 0.06 eV/$\mathring{A}$. For comparison, a non-spin polarized (NSP) calculation is also performed for each case. The energy reduction due to spin polarization for all surfaces with a magnetic ground-state is shown in Table I. It has been obtained as the total energy difference between the relaxed SP and NSP slabs. The large values in the table are in the range of those obtained for magnetic bulk oxides [14], and should not be taken as an exact prediction of the actual values, but as a correct description of the order of magnitude and global trend.

Table II summarizes our first main result. It shows the total magnetic moments at the surface O plane for all the structures which present a magnetic ground state, together with their in-plane ($||$) and normal ($\perp$) p projections onto the surface. All spin moments arise almost exclusively from the p electrons at the valence band of the oxide. They reach large values, ranging from 0.8 to 1.6 μ_B. Notice that only the O-rich oxide surfaces are magnetic. Both the cation-ended and the non-polar O surfaces not in the table do not show any spin polarization. The distinct characteristic of all these magnetic structures is that they are polar divergent surfaces [20] with a loss of cationic coordination for the outermost O atoms. This already suggests that the O spin polarization is intimately related to the decrease of the oxygen ionic charge at the surface with respect to the bulk. The correlation is evident after inspection of Table II, where the rightmost columns provide the O Mulliken populations at the surface layer and the bulk. In all these cases the surface O lose ionic charge approaching a charge neutral state. Moreover, the smaller the oxygen ionic charge, the larger its associated magnetic moment.

Indeed, for the calculated surfaces with a non-magnetic ground state we obtain O charges close to the bulk ones. An example is given in table III, which compares the layer resolved Mulliken populations and moments for the two O-ended c-ZrO_2(111) surfaces. ¿From the results for c-$ZrO_2(111)_{O-O-}$ in table III, we can again observe the clear correlation between the reduction of the ionic charge and the size of the magnetic moment. This means that the spin polarization is a response of the system to the loss of transferred charge. Even if the magnetization is a local effect, rooted in the lack of donor electrons for the outermost O atoms, the interaction of these atoms with the lower adjacent planes cannot be neglected: the spin polarization at the surface layer induces a magnetic moment at the neighbouring planes, which decays as we deepen into the bulk.

Our second main result is the finding that all magnetic surfaces are half-metallic. Half-metals are strong candidates for the development of spintronic devices, as they can naturally produce electronic currents of well-defined spin polarization [21]. Figure 1 shows the density of states (DOS) at the three uppermost layers and the bulk for two representative Al_2O_3(0001) and c-ZrO_2(001) surfaces, both for SP (left) and NSP (right) calculations. In all the magnetic structures investigated, the Fermi level (E_F) crosses the valence band of the topmost layer, although some surfaces present a very localized minimum at E_F, as occurs in Al_2O_3(0001). Remarkably, the bands crossing E_F have always a well defined spin polarization, the majority spin states being full while the minority spin band is partially filled. The result, common to all the magnetic surfaces studied here, is a half-metallic system.

The differences between the magnetic surfaces manifest in the details of the electronic distributions. This can be best observed regarding the shape of the DOS in figure 1. For c-ZrO_2(001), the DOS at the topmost O plane is bulk-like except for the usual surface narrowing, both for the SP and NSP calculations. The effect of the spin exchange is mostly the shift of the minority spin band. At the SP Al_2O_3(0001) surface, the most significant effect is the reduction of the DOS at E_F, something also observed at c-$ZrO_2(111)_{O-O-}$ and MgO(111). For these surfaces, the shape of the majority spin DOS is almost bulk-like, while a deep redistribution of charge affects the minority spin electrons.

The major changes observed in the minority spin DOS are also present in the spatial charge distributions. This can be directly seen in the left and central panels of figure 2, which depict the spin resolved charge density differences (CDD, total charge density minus the superposition of atomic charge densities) of the MgO(111) and c-$ZrO_2(111)_{O-O-}$ surfaces, within a plane normal to the surface along the bond direction between a surface O atom and a nearest neighbour at the layer below. The majority spin band being completely filled, as was shown in the DOS, the corresponding CDD adopts the spherical symmetry of the bulk. On the contrary, anisotropic lobular shapes appear in the minority charge. This assymetry between the spatial distributions of the spin states is a common feature to all the magnetic structures studied here, although the effect is specially relevant for the surfaces shown in figure 2. The rightmost panels of the figure show the corresponding spin density difference (SDD), CDD of majority spin minus CDD of minority spin. The crystal field induces a high directionality of the spin moments, involving orbitals along specific directions. For the c-$ZrO_2(111)_{O-O-}$ and MgO(111) systems this leads to a highly anisotropic distribution of the magnetic charge, also evidenced in the $m_{||}$ and $m_{\perp}$ projections of table II. The specific dominant distribution depends on the particular structure: contained within the surface plane for c-$ZrO_2(111)_{O-O-}$ and normal to the surface for MgO(111).

Finally, some considerations about energetics should be mentioned. To analyze the surface energetics requires to consider all mechanisms which stabilize the surfaces under study [4, 25], a huge task beyond the scope of this work. Nevertheless, it is well known that bulk metastable terminations coexist in grain boundaries, and they even become energetically favourable in ultrathin films and nanostructures [24]. Based on thermodynamic arguments [22, 23], the surface energy of the polar surfaces under study may be lowered below that of the corresponding non-polar terminations under high O pressures when the spin polarization is included. On the other hand, we have also performed preliminar studies of the effect of Zr vacancies in bulk ZrO_2 that confirm the existence of the magnetization mechanism presented here. Similar conclusions have been reported for bulk HfO_2 in the presence of Hf vacancies [26].

In conclusion, we have proved the existence of local magnetism at the ideal O-ended polar surfaces of ceramic oxides. Large spin moments are formed at the outermost surface plane due to the lack of donor charge and the subsequent creation of $2p$ holes in the valence band of the oxide. This leads to a half-metallic ground state, with the majority spin band completely filled and only minority spin states at the Fermi level. The orientation of the magnetic moment with respect to the surface plane can be tuned selecting adequate crystal orientations. The fact that polar surfaces of nonmagnetic materials with large bulk bandgap exhibit a 100 % spin polarization at the Fermi level opens a new route to the manipulation of spin currents. In fact, the mechanism presented here can explain the unexpected magnetism measured in thin films of HfO_2 and ZrO_2 [8, 9], relating it to the existence of cation defects. Even more, the present ability to produce ultrathin films and nanometric grains of these materials make feasible the fine control of their structure and stoichiometry, implying the possibility to extend this surface magnetism to any low-dimensional configuration.

This work has been partially financed by the Spanish Ministerio de Educación y Ciencia and the DGICyT under contracts MAT2003-04278, MAT2004-05348 and CAM2004-0440, and by the Ramón y Cajal program. J.I. B. acknowledges financial support from the I3P program of the CSIC.

[1] G.V. Hansson and R.I.G. Uhrberg, *Surf. Sci. Rep.* **9**, 197 (1988); J.A. Kubby and J.J. Boland *Surf. Sci. Rep.* **26**, 61 (1996).
[2] P. Crespo *et al*, *Phys. Rev. Lett.* **93**, 087204 (2004); Y. Yamamoto *et al*, *Phys. Rev. Lett.* **93**, 116801 (2004).
[3] H. Li and B.P. Tonner *Phys. Rev. B* **40**, 10241 (1989); C.R. Aita, *Nanostruct. Mater.* **4**, 257 (1994); F. Bisio *et al*, *Phys. Rev. Lett.* **93**, 106103 (2004).
[4] C. Noguera, *J. Phys.: Condens. Matter* **12**, R367 (2000), and references therein.
[5] S.A. Wolf *et al*, *Science*, **294**, 1488 (2001).
[6] G.A. Prinz, *Science*, **282**, 1660 (1998).
[7] L. Du *et al*, *Surf. and Coatings Technology* **192**, 311 (2005); S.P. Parkin *et al*, *Nature Materials* **3**, 862 (2004); Y.-M. Sun *et al*, *Applied Surf. Sci.* **161**, 115 (2000); M.A. Schofield *et al*, *Thin Solid Films* **326**, 106 (1998).
[8] M. Venkatesan, C.B. Fitzgerald, and J.M.D. Coey, *Nature* **430**, 630 (2004).
[9] M. Coey, Abstract U5.00005 of 2005 APS March Meeting.
[10] Y. Matsumoto *et al*, *Science* **291**, 854 (2001); S.B. Ogale *et al*, *Phys. Rev. Lett.* **91**, 077205 (2003); M. Venkatesan, C.B. Fitzgerald, J.G. Lunney, and J.M.D. Coey, *Phys. Rev. Lett.* **93**, 177206 (2004).
[11] I.S. Elfimov, S. Yunoki, and G.A. Sawatzky, *Phys. Rev. Lett.* **89**, 216403 (2002).
[12] L.S. Dorneles *et al*, *Appl. Phys. Lett.* **85**, 6377 (2004).
[13] J.P. Perdew *et al.*, *Phys. Rev. B* **46**, 6671 (1992).
[14] A. Rohrbach, J. Hafner, and G. Kresse, *Phys. Rev. B* **70**, 125426 (2004); D. Kodderitzsch *et al*, *Phys. Rev. B* **66**, 064434 (2002); X. Feng, *Phys. Rev. B* **69**, 155107 (2004).

TABLE I: Energy reduction (eV/M_xO_y unit) of the SP relaxed slab with respect to the corresponding NSP case for all magnetic surfaces under study.

	ZrO_2			Al_2O_3	MgO
c-$(111)_{O-O-}$	m-(001)	t-(001)	c-(001)	(0001)	(111)
0.91	0.44	0.22	0.22	1.37	0.44

TABLE II: Spin moments (in μ_B) at the topmost layer of the surfaces of Table I, together with the decomposition of the p orbital contribution parallel and normal to the surface plane. The rightmost columns provide the corresponding Mulliken charge populations (Q) compared to the inner bulk value (Q_b). The O_1 and O_2 entries for the non-cubic ZrO_2 structures refer to the two inequivalent in-plane positions.

Surface	$\mathbf{m}_{tot}$	$m^p{}_{\|\|}$	$m^p{}_{\perp}$	**Q**	Q_b
c-$ZrO_2(111)_{O-O-}$	**1.56**	1.50	0.04	**6.02**	6.79
m-ZrO_2(001)-O_1	**1.43**	0.81	0.61	**6.10**	6.66
-O_2	**1.43**	0.81	0.60	**6.11**	
t-ZrO_2(001)-O_1	**1.19**	0.54	0.64	**6.13**	6.76
-O_2	**0.59**	0.55	0.03	**6.17**	
c-ZrO_2(001)	**0.83**	0.62	0.21	**6.29**	6.79
Al_2O_3(0001)	**0.97**	0.74	0.23	**6.10**	6.49
MgO(111)	**0.83**	0.06	0.76	**6.37**	6.72

[15] B. Kralik, E.K. Chang, and S.G. Louie, *Phys. Rev. B* **57**, 7027 (1998).
[16] H.J.F. Jansen, *Phys. Rev. B* **43**, 7267 (1991); A. Eichler, *Phys. Rev. B* **64**, 174103 (2001); X. Zhao and D. Vanderblit, *Phys. Rev. B* **65**, 075105 (2002).
[17] P. Ordejón, E. Artacho, and J.M. Soler, *Phys. Rev. B* **53**, R10441 (1996); J.M Soler *et al.*, *J. Phys.: Condens. Matter* **14**, 2745 (2002).
[18] J.I. Beltrán *et al.*, *Phys. Rev. B* **68**, 075401 (2003).
[19] C.J. Howard, R.J. Hill, and B.E. Reichert, *Acta Crystallogr. Sect. B: Struct. Sci.* **44**, 116 (1988).
[20] P.W. Tasker, *J. Phys. C: Sol. State Phys.* **12**, 4977 (1979).
[21] R.A. de Groot, F.M. Müller, P.G. van Engen, and K.H.J. Buschow, *Phys. Rev. Lett.* **50**,2024 (1983).
[22] I.G. Batyrev, A. Alavi, and M.W. Finnis, *Phys. Rev.B* **62**, 4698 (2000).
[23] A. Eichler and G. Kresse, *Phys. Rev. B* **69**, 045402 (2004).
[24] S. Mahieu *et al*, *J. Cryst. Growth* **279**, 100 (2005); K. Meinel, K.-M. Schindler, and H. Neddermeyer, *Surf. Sci.* **532-535**, 420 (2003); G. Baldinozzi *et al*, *Phys. Rev. Lett.* **90**, 216103 (2003).
[25] O. Dulub, U. Diebold, and G. Kresse, *Phys. Rev. Lett.* **90**, 016102 (2003).
[26] C. Das Pemmaraju and S. Sanvito, *Phys. Rev. Lett.* **94**, 217205 (2005).

FIG. 1: DOS for the three topmost planes and the bulk of Al_2O_3(0001) and c-ZrO_2(001) after SP (left) and NSP (right) calculations. Positive (negative) values correspond to majority (minority) spin states. Energies are referred to the Fermi level. The total spin moments at each layer are indicated for the SP case.

TABLE III: Layer resolved spin moments (in μ_B) and Mulliken populations for the O-ended c-ZrO_2(111) surfaces. The layers, labelled according to their composition, are ordered from the surface (top row) to the bulk.

Layer	*O-O-*		*O-Zr-*	
	m_{tot}	Q	m_{tot}	Q
O	1.56	6.02		
O	0.47	6.57	–	6.68
Zr	-0.13	2.60	–	2.49
O	0.07	6.79	–	6.79

FIG. 2: Left and middle panels: spin resolved CDD for the (top) MgO(111) and (bottom) c-$ZrO_2(111)_{O-O-}$ surfaces. Right panels: corresponding SDD.

MgO(111)

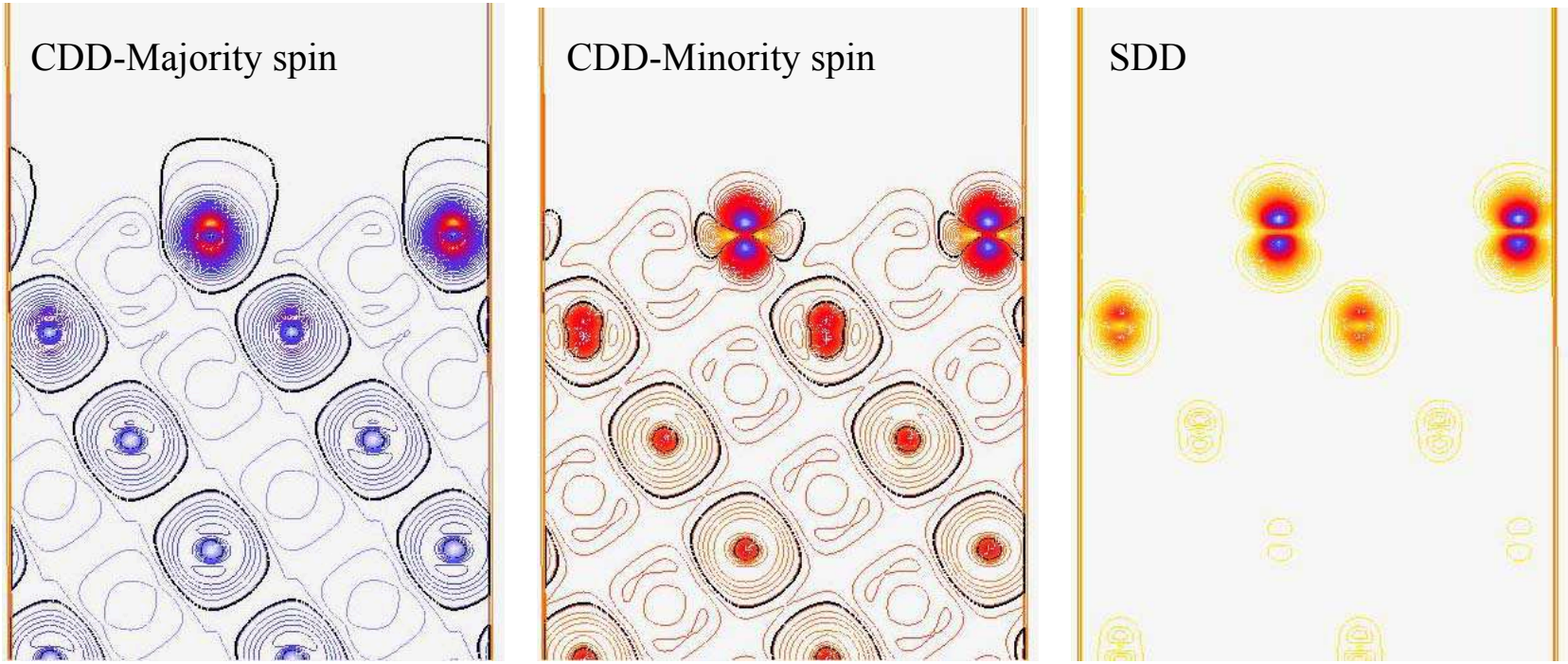

c-$ZrO_2(111)_{O\text{-}O}$